A study in spherical accretion of self-gravitating fluids in a general relativistic framework

M. C. Richter

Thesis Presented for the Degree of

DOCTOR OF PHILOSOPHY

Centre for Theoretical Physics and Astrophysics

Department of Physics

UNIVERSITY OF CAPE TOWN

November 26, 2010

Abstract

A new general framework for studying relativistic spherical accretion of a self-gravitating fluid onto a central black hole is introduced in stationary coordinates for an observer at infinity. The important feature of gravitational backreaction due to a self-gravitating fluid on the metric is included in the model. The model is solved numerically for the most simple case of a polytropic fluid and compared to analytical solutions, which the model approximates in the "test-fluid" limit, and the implications of these findings are discussed. The findings for the test case comparison are favourable with good agreement. Finally, the model is focused on the accretion of a relativistic Fermi gas and the implications this might have on the rapid growth of supermassive black holes from clouds of sterile neutrino dark matter in the early universe. The results give good agreement with a Newtonian model of supermassive black hole growth called the symbiotic scenario.

Contents

Chapter 1

Introduction

The idea of fundamental forces pervade the understanding of the way the universe works; from the strong and weak interactions in the subatomic world, the electromagnetic force in the microscopic realm to gravity acting from the familiar scales to galactic and cosmic proportions. When gravity is the dominating force, as it is at these relatively large and extremely vast distances of the scale of solar systems, galaxies, galaxy clusters and beyond, the idea of attraction is a fundamental concept one must keep in mind; that is how gravity works. Since this attraction is the only way gravity has been observed to work, accretion is a rather fundamental feature of gravitational systems, seen all throughout the universe and powers the most luminous and energetic objects seen in the cosmos. Protostellar clusters grow to become fully fledged solar systems, gas clouds collapse to form stars and black holes and some of those black holes become active galactic nuclei (AGN) and the enormously massive quasars. When these behemoths pull matter onto their event horizon the process has the highest efficiency rate of conversion of mass energy to radiation known to science, and is responsible for their incredible luminosity. Gravitational accretion of matter is the fundamental building process involved in all these scenarios and is powered by gravity. The more we understand about this building process of accretion the better we can understand some of the most energetic objects and processes observed in the cosmos, lurking at the center

of galaxies. This thesis aims to extend the body of knowledge of the accretion process for relativistic matter.

The original treatment of spherically symmetric accretion was made by Lyttleton, Hoyle and Bondi [1, 2, 3] which involved a massive particle traveling through a gaseous medium and accumulating or accreting the surrounding matter, working with Newtonian principles and a Keplerian gravitational potential. As such, the treatment proved to be useful in working on a number of astrophysical phenomena such as binary clusters, protostellar cluster accretion and galaxy cluster accretion. Bondi then released his work that treated the accretion process as a hydrodynamical problem [4], where a test fluid of negligible mass accreted onto a central dominating body in a steady flow of matter onto a central accreting object. This was still done in a Newtonian framework. The departure from such a Newtonian treatment to a more general-relativistic treatment was made by Michel [5] and then later summarised in the textbook by Shapiro and Teucholsky [6] in which the hydrodynamical problem is placed into a Schwarzschild spacetime, however the test fluid of negligible mass employed by Bondi is still used. Under this simplification, the analysis yielded a stable steady flow exhibiting transonicity. In the case of a black hole central body, this critical transonic point would always lie outside the event horizon [5]. This test fluid treatment of the accretion problem simplified the analysis and showed vital characteristics of a steady state flow, however it omitted the effect the accreted test fluid has on the spacetime surrounding the central body. In the most simple case, such as for a polytropic equation of state, the relativistic picture with a test fluid can be solved analytically as was done by Babichev et al [7, 8]. The backreaction on the metric due to the accreting fluid has been investigated by Malec et al [9, 10] in a co-moving coordinate frame. Other than the aforementioned work, there seems to be little analysis of the relativistic accretion problem with a fixed observer that includes the backreaction, as opposed to the co-moving coordinate frame more commonly used in accretion studies. This begs the development of exactly such a theory, as it has numerous potential applications in astrophysics and cosmological physics and delivers a useful starting point for comparison to observation. Such a fixed coordinate

frame would also be useful as it shares many similarities to previous studies of accretion that neglect the backreaction of the surrounding fluid, and is thus comparisons are easily made.

The fundamental feature of backreaction is not usually necessary in models of accretion that describe systems like planetary disks around young stars or even the accretion disks found in cataclysmic variables and X-ray binaries, as the accreting fluid comprises a trivial fraction of the total mass of the system and can be neglected. In the proposed model of supermassive black hole growth called the symbiotic scenario, summarised below, the accreting fluid becomes the dominating contribution to the total mass of the system and the backreaction becomes a conceptually important feature of the accretion process and requires some study.

1.1 Motivation set forth by the symbiotic scenario

An important application of such a relativistic accretion theory is the study of the origin of quasars and active galactic nuclei, which are believed to be supermassive black holes (SMBH). The process by which these gargantuan objects grow to such vast sizes is poorly understood. There are many gaps in the knowledge regarding the origin of SMBHs, some more massive than three billion of our Suns combined. The most puzzling observation of the early universe is that these SMBHs are observed at red-shift values of $z = 6.41$ [11] which corresponds to a time of $t = 850$ million years (Myr) after the Big Bang. What is puzzling about this observation is that this early appearance cannot be reconciled with a theoretical picture of a solar mass black hole growing to a supermassive size by accreting ordinary baryonic matter. That kind of accretion is limited in growth rate by the Eddington limit that bounds the infall of ionizing matter due to emission of radiation. Calculations of such growth times yields a prediction for the emergence of SMBHs of at least twice that which is observed. Further confounding evidence is given by the observation that SMBHs in the form of quasars emerge much earlier than the smaller scale SMBH observed as AGN, seemingly pointing

to an anti-hierarchical nature of the accretion process; also poorly explained by many contemporary theories.

Solutions to these problems concerning the early formation of SMBHs are proposed by the symbiotic scenario set out in [12], whereby the ordinary solar mass seed black holes grow to the supermassive scale by accreting dark matter. In this theory, the dark matter is composed of degenerate sterile neutrinos that form supermassive structures early in the universe. Baryonic matter, in the form of molecular hydrogen clouds, interacts gravitationally with the dark matter sterile neutrinos, and easily coalesces at the center of these proposed sterile neutrino balls. This way a large star can easily form and eventually undergo gravitational collapse to form a black hole of the scale of several solar masses. This seed black hole would then accrete the surrounding sterile neutrino dark matter. Now it is clear to see that this scenario sets the scene for a central accretor of negligible mass compared to a supermassive fluid of degenerate sterile neutrinos surrounding it.

The process of accretion of the sterile neutrinos is unhampered by the Eddington limit, as the particles only interact gravitationally, and so the central body can grow much quicker than it could accreting ordinary baryonic matter. Calculations of the accretion rate within a non-relativistic theory agree well with the early appearance of the quasars mentioned above. This Newtonian theory has its limits, as the calculations of the accretion rate break down for black hole masses close to the Oppenheimer-Volkoff limit for degenerate systems. To make more precise predictions for this symbiotic scenario, the underlying accretion theory should be general relativistic.

1.2 The symbiotic scenario in review

To give a brief overview of the symbiotic scenario, it is important to declare the premise of the theory. The model proposes a candidate particle for dark matter in the form of a degenerate sterile neutrino that forms part of a renormalisable extension of the minimal standard model called νMSM [13, 14, 15]. In this extension of the standard

model, three new "sterile" neutrino particles are introduced: two particles with masses larger than the proton mass, and one light particle with mass of the order $m_\nu \sim 10$ keV$/c^2$. These neutrinos are called sterile since they interact with the ordinary neutrinos through an extremely small mixing angle. This limited interaction is what makes the lightest of the three sterile neutrinos quasi-stable, bestowing it with a lifetime of $\tau\left(\nu_s \rightarrow \nu_e\, \nu\bar{\nu}\right) = 1.21 \times 10^{19}$ yr, larger than the current age of the universe [16].

Choosing a large lepton asymmetry of the order $L_\nu = 10^{-2}$, consistent with the number of three active neutrinos at nucleosynthesis [17], means the sterile neutrinos would be created through non-resonant [18, 19, 20, 21] and resonant scattering [16, 22, 23, 24] of the active neutrinos. The two production processes would ensure the creation of high-energy sterile neutrinos, interpreted as warm dark matter [25], and sterile neutrinos of lower energy, taken to be cool dark matter. The cool dark matter would be prone to cluster in small gravitational potential wells, and grow to large neutrino balls [26, 27, 28, 29, 30]. The Oppenheimer-Volkoff (OV) mass limit [31, 32] of such a system of degenerate fermions would be

$$M_{\mathrm{OV}} = 2.778 \times 10^9 M_\odot \left(\frac{15\ \mathrm{keV}}{m_\nu c^2}\right)^2 \left(\frac{2}{g}\right)^{1/2}, \tag{1.1}$$

and represents the maximum size of such a sterile neutrino ball, above which, the gravitational pull of the mass overcomes the degeneracy pressure of the neutrinos, and the ball collapses to a black hole.

Once these neutrino balls have formed it is proposed that they could easily accumulate molecular hydrogen at their center, as these structures would possess gravitational potential wells that essentially act like an harmonic oscillator potential. This means that the center of these neutrino balls would be perfect breeding grounds for large stars, that would eventually burn out and collapse to stellar-mass black holes. As soon as a black hole resides at the center of a sterile neutrino ball, the former would start accreting the surrounding neutrino fluid. This process of producing large stars would be accelerated for neutrino balls close to the OV-limit as opposed to smaller size struc-

tures and gives a valid explanation for the anti-hierarchical formation of quasars and the AGN.

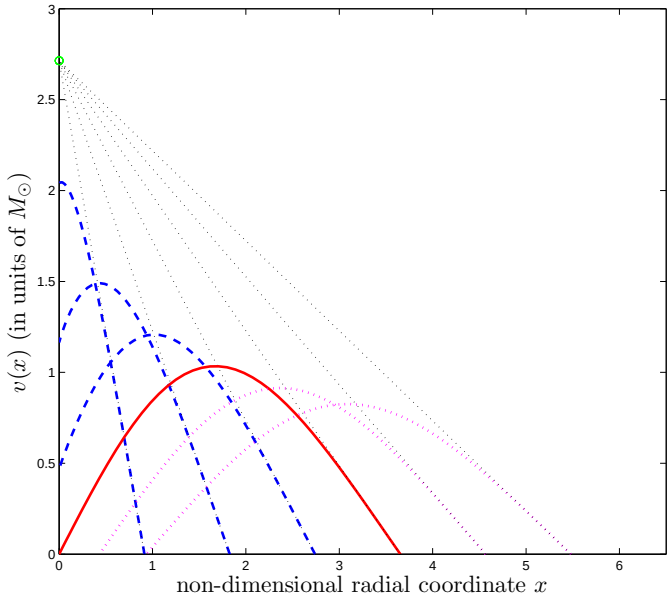

Figure 1.1: The Lane-Emden solutions: We see here the M-type (blue-dashed), E-type (red-solid) and F-type (magenta-dotted) solutions. All solutions have the total mass $M = m_C + m_H = 2.71406\ M_\odot$.

In the non-relativistic static model, the gravitational potential of the sterile neutrino ball can be described by the Lane-Emden equation with appropriate boundary conditions and thus all important quantities can be calculated numerically. Two types of solution of the Lane-Emden equation are of physical interest: the E-solution that represents a fermionic fluid with no mass at the center and the M-solutions that represents the case of a central body surrounded by a halo of fluid, depicted in Fig. 1.1. Since this is a static model, the solutions of the Lane-Emden equation represent snapshots of the accretion process at different stages. The scaling properties of the Lane-Emden equation allow the solutions to also be scaled appropriately and calculations of the accretion rate can be made for the mass scales of the sterile neutrino balls. The accretion

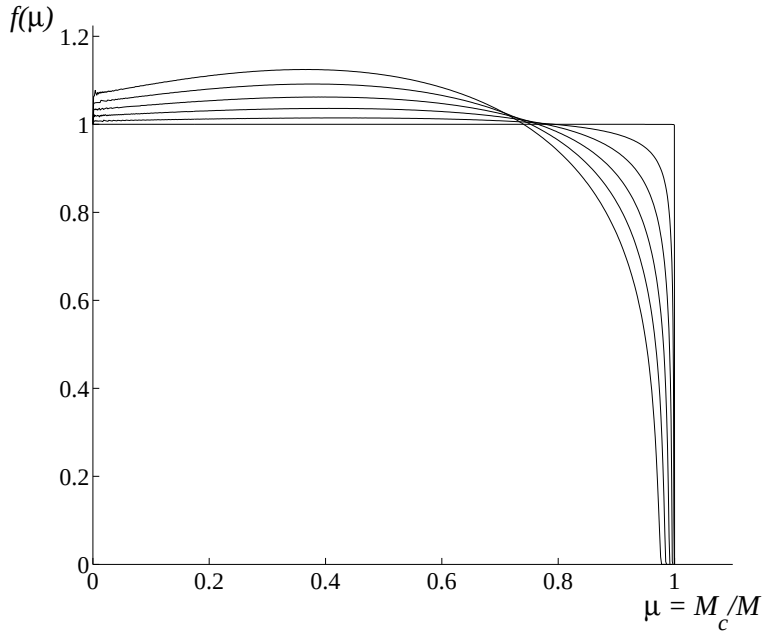

Figure 1.2: Various shut-off parameters $f(m_C)$ for different values of the ratio m_C/M. We see a range of total mass varying from $M = 10^6 M_\odot$ for the box shaped function to $M = 10^9 M_\odot$ for the curve with the largest maximum.

rate formula becomes

$$\dot{M} = \frac{f(m_C)}{\tau_A} m_C^2, \tag{1.2}$$

where, τ_A is the characteristic accretion time, $f(m_C)$ is calculated numerically and shown in Fig. 1.2, hint at the possibility that such a theory can give an explanation for the rapid growth of SMBHs in the early universe, giving a growth time of < 5 Myr for a black hole from solar mass scale to a mass of $3 \times 10^6 M_\odot$, having almost completely consumed the sterile neutrino ball. This results in a predicted appearance of quasars driven by SMBHs 800 to 850 Myr after the Big Bang, in accordance with observation. The non-relativistic theory works well for black hole masses well below the OV-limit, of the order $\lesssim 10^6 M_\odot$, but breaks down for masses approaching the said upper bound. At this point the subject of this thesis takes over in tackling the problem of a fully relativistic approach to spherical accretion including the backreaction of the surrounding fluid.

Chapter 2

Theoretical framework of the relativistic accretion theory

2.1 Relativistic accretion flow analysis

This section introduces the theoretical work done by Michel [5] and later summarised by Shapiro & Teukolsky [6] and aims to lay the foundation for the derivation of the analytical solution for the ultrarelativistic stiff matter in the next section.

The simplifying assumption of a dominating central object accreting a test fluid of negligible mass must be made in order to perform the analysis. This means that the Schwarzschild spacetime geometry, as well as the corresponding metric tensor, may be used since the backreaction of the accreted fluid on the metric is neglected.

Starting from the mass conservation equation $J^{\mu}_{;\mu} = 0$ and energy conservation equation $T^{\mu}_{0;\mu} = 0$ of a perfect fluid with stress-energy tensor $T_{\mu}{}^{\nu} = (\rho + P)\, U_{\mu}U^{\nu} - \delta_{\mu}{}^{\nu}P$ and integrating under steady state conditions and assuming spherical symmetry, the equations

$$nU^{r}\sqrt{-g} = k_1, \tag{2.1}$$

$$(\rho + P)U_0U^{r}\sqrt{-g} = k_2, \tag{2.2}$$

become apparent. Here n is the particle number density making up the rest-mass energy

density mn, $\rho = mn + \epsilon$ is the total proper energy density with internal energy ϵ and P is the proper pressure. The setting for these calculations is the Schwarzschild metric

$$ds^2 = e^{\nu}dt^2 - e^{\lambda}dr^2 - r^2\left(d\theta^2 + \sin^2\theta d\phi^2\right), \tag{2.3}$$

with units of $c = 1$, thus $U_\mu U^\mu = 1$, and metric functions for the exterior Schwarzschild solution are

$$e^{\nu} = e^{-\lambda} = 1 - \frac{2GM}{r} = 1 - \frac{2m}{r}, \tag{2.4}$$

where the mass is replaced by the variable $m = GM$ and the determinant of the metric is given by $g = -r^4\sin^2\theta$. This gives the set of equations

$$n\,U\,r^2 = k_1, \tag{2.5}$$

$$\left(\frac{\rho + P}{n}\right)^2\left(1 - \frac{2m}{r} + U^2\right) = k_3. \tag{2.6}$$

Here, the velocity $U = U^r$ and Eq. (2.6) is the result of taking Eq. (2.2), dividing by (2.1) and squaring. Now differentiating Eqs. (2.5) and (2.6) and eliminating $d\rho$ gives

$$\left[2c_S^2 - \frac{m}{r}\left(1 - \frac{2m}{r} + U^2\right)^{-1}\right]\frac{dU}{U} + \left[c_S^2 - U^2\left(1 - \frac{2m}{r} + U^2\right)^{-1}\right]\frac{dr}{r} = 0, \tag{2.7}$$

where the speed of sound is defined to be

$$c_S^2 = \frac{dP}{d\rho} = \frac{n}{\rho + P}\frac{dP}{dn}. \tag{2.8}$$

Setting the bracketed expressions in Eq. (2.7) to zero gives the location of the critical point of the flow where the fluid becomes transonic, i.e. moving from a subsonic inflow of matter to a supersonic regime. Thus

$$U_*^2 = \frac{m}{2r_*}, \tag{2.9}$$

$$c_{S*}^2 = \frac{U_*^2}{1 - 3U_*^2}. \tag{2.10}$$

This analysis gives the assurance that such a critical point will always lie outside of a central horizon of a collapsed object such as a black hole situated at $r = 2m$ since c_S^2 must be positive in all physical cases, which constrains $U_*^2 < 1/3$ and hence also $r_* > 6m$.

2.2 Recent progress in gravitational accretion

Moving on to a more recent analysis of the accretion problem, it is useful to examine work by Babichev *et al* [7, 8] where the authors have worked out analytical solutions for accretion of a "test fluid" with linear equation of state. This would make an interesting test case for the model laid out in this thesis. The starting point of the calculation assumes a Schwarzschild metric as in the last section given by Eq. (2.3) as the fluid is falling onto a black hole. Similar to the calculation in [5], energy-momentum conservation of a perfect fluid $T^{\mu\nu}_{;\nu}$ gives

$$(\rho + P)\left(1 - \frac{2m}{r} + U^2\right) r^2 U = C_1, \tag{2.11}$$

where ρ, P, m, r and $U = U^r$ are defined as before. The projection of the energy conservation equation onto the 4-velocity U_μ gives

$$U^\mu \rho_{,\mu} + (\rho + P) U^\mu_{;\mu} = 0, \tag{2.12}$$

and upon integration gives

$$r^2\, U\, \exp\left(\int \frac{d\rho'}{\rho' + P}\right) = -A. \tag{2.13}$$

Since this model is dealing with infalling matter, $U < 0$ and the integration constant $A > 0$. This is a generalisation of the work done by Michel [5] as there is no use of the particle conservation law. Continuing with the calculation, the radial projection of the relativistic Euler's equation results in the relation

$$\sqrt{U^2 + 1 - \frac{2m}{r}}\, \exp\left(\int \frac{d\rho'}{\rho' + P}\right) = B. \tag{2.14}$$

It is possible to calculate the density and flow velocity as a function of the radius by defining the equation of state relating the pressure P and the density ρ. Choosing a linear equation of state such that $P = w\rho$, which models ultrarelativistic stiff matter for $w = 1$ and radiation for $w = 1/3$, the exponential in Eqs. (2.13) and (2.14) becomes

$$\exp\left(\int \frac{d\rho'}{\rho' + P}\right) = \rho^{\frac{1}{1+w}}. \tag{2.15}$$

In the case of $w = 1$, combining Eqs. (2.13), (2.14) and (2.15) and eliminating the density $\rho(r)$ yields the analytical solutions for radial flow velocity $U(r)$ and from this the density $\rho(r)$, which are given by

$$U(r) = \frac{R_s^2}{\sqrt{r\,(r+R_s)\,(r^2+R_s^2)}}, \tag{2.16}$$

$$\frac{\rho(r)}{\rho_\infty} = \left(1+\frac{R_s}{r}\right)\left(1+\left(\frac{R_s}{r}\right)^2\right). \tag{2.17}$$

In these relations, ρ_∞ is the density very far away and $R_s = 2GM$ is the Schwarzschild radius of the central dominating object, where the constants of integration are evaluated to be $A = R_s^2 B$ and $B^2 = \rho_\infty$.

For the case of $w = 1/3$, the calculation of the flow velocity $U(r)$ is similar but the calculation to find the density becomes less trivial and the result is taken directly from [7], which gives the density as a function of radius to be

$$\frac{\rho}{\rho_\infty} = \left[z + \frac{r}{3\,(r-R_s)}\right]^2, \tag{2.18}$$

where

$$z = \begin{cases} 2\sqrt{\frac{a}{3}}\cos\left(\frac{2\pi}{3}-\frac{\beta}{3}\right), & 2 \le r/GM \le 3 \\ 2\sqrt{\frac{a}{3}}\cos\left(\frac{\beta}{3}\right), & r/GM > 3, \end{cases}$$

$$\beta = \arccos\left[\frac{b}{2(a/3)^{3/2}}\right],$$

and

$$a = \frac{r^2}{3\,(r-R_s)^2}, \qquad b = \frac{2r^3}{27\,(r-R_s)^3} - \frac{108}{(r-R_s)\,r^3}.$$

2.3 Calculations from the metric

To describe the accretion of a perfect fluid in a stationary model, simplifications can be made early on before any calculations are made, such as the stipulation of spherical symmetry, as that is the most simple case of matter distribution. Therefore it is prudent to consider a timelike coordinate t and three spacelike coordinates r, θ and ϕ. The most

general line element for such a spherically symmetric configuration of matter has the well known form

$$ds^2 = e^{\nu}dt^2 - e^{\lambda}dr^2 - r^2\left(d\theta^2 + \sin^2\theta d\phi^2\right), \tag{2.19}$$

(with units of $c = 1$). In this instance, to maintain generality for the stationary flow, the metric functions $\nu = \nu(r,t)$ and $\lambda = \lambda(r,t)$ are functions of both time t and the radial coordinate r. The subsequent metric tensor is worked out through the relation to the line element, such that

$$ds^2 = g_{\mu\nu}dx^{\mu}dx^{\nu} \tag{2.20}$$

and thus the metric tensor is given in the matrix form as

$$g_{\mu\nu} = \begin{pmatrix} e^{\nu} & 0 & 0 & 0 \\ 0 & -e^{\lambda} & 0 & 0 \\ 0 & 0 & -r^2 & 0 \\ 0 & 0 & 0 & -r^2\sin^2\theta \end{pmatrix} \tag{2.21}$$

The equations of motion for a free-falling particle in this gravitational spacetime will be given by the Einstein field equations

$$\begin{aligned} 8\pi G\, T_{\mu\nu} &= G_{\mu\nu} + \Lambda g_{\mu\nu} \\ &= R_{\mu\nu} - \frac{1}{2}Rg_{\mu\nu} + \Lambda g_{\mu\nu}. \end{aligned} \tag{2.22}$$

In this formulation, the Einstein tensor $G_{\mu\nu}$, given in terms of the Ricci tensor $R_{\mu\nu}$ and Ricci scalar R, is required to be calculated and the energy-momentum tensor $T_{\mu\nu}$ will be imposed with consideration to the matter content of the system. For this particular case of fluid accretion, the cosmological constant will be set to zero, $\Lambda = 0$. To find the components of the Einstein tensor $G_{\mu\nu}$, start with the Riemann curvature tensor $R^{\rho}{}_{\sigma\mu\nu}$, which is given in terms of the Christoffel symbols or connection coefficients by

$$R^{\rho}{}_{\sigma\mu\nu} = \partial_{\mu}\Gamma^{\rho}{}_{\nu\sigma} - \partial_{\nu}\Gamma^{\rho}{}_{\mu\sigma} + \Gamma^{\rho}{}_{\mu\lambda}\Gamma^{\lambda}{}_{\nu\sigma} - \Gamma^{\rho}{}_{\nu\lambda}\Gamma^{\lambda}{}_{\mu\sigma}, \tag{2.23}$$

where $\partial_{\mu} = \partial/\partial x_{\mu}$ are the coordinate vector fields and the connection coefficients are given by

$$\Gamma^{\alpha}_{\mu\nu} = \frac{1}{2}g^{\alpha\beta}\left(g_{\beta\mu,\nu} + g_{\beta\nu,\mu} - g_{\mu\nu,\beta}\right). \tag{2.24}$$

The Ricci tensor is worked out from the Riemann tensor by the contraction of the first and third indices, like

$$R_{\mu\nu} = R^{\alpha}_{\ \mu\alpha\nu}, \tag{2.25}$$

and the Ricci scalar by a product of the Ricci tensor with the contravariant metric tensor

$$R = g^{\mu\nu} R_{\mu\nu}. \tag{2.26}$$

Following the workings of [33], the non-zero connection coefficients can be worked out to be

$$\begin{array}{lll}
\Gamma^{r}_{\ rr} = \frac{\lambda'}{2}, & \Gamma^{0}_{\ r0} = \frac{\nu'}{2}, & \Gamma^{\theta}_{\ \phi\phi} = -\sin\theta\cos\theta, \\
\Gamma^{0}_{\ rr} = \frac{\dot{\lambda}}{2} e^{\lambda-\nu}, & \Gamma^{r}_{\ \theta\theta} = -r e^{-\lambda}, & \Gamma^{r}_{\ 00} = \frac{\nu'}{2} e^{\nu-\lambda}, \\
\Gamma^{\theta}_{\ r\theta} = \frac{1}{r}, & \Gamma^{\phi}_{\ r\phi} = \frac{1}{r}, & \Gamma^{\phi}_{\ \theta\phi} = \cot\theta, \\
\Gamma^{0}_{\ 00} = \frac{\dot{\nu}}{2}, & \Gamma^{r}_{\ r0} = \frac{\dot{\lambda}}{2}, & \Gamma^{r}_{\ \phi\phi} = -r\sin^2\theta e^{-\lambda},
\end{array}$$

where the connection coefficients are symmetric in the lower two indices and radial derivatives are denoted by a raised prime (x') and time derivatives by a raised dot ($\dot{x}$). Subsequently, the non-trivial Einstein field equations that are unpacked from the terse tensor notation are

$$8\pi G\, T_0^{\ 0} = \frac{1}{r^2} - e^{-\lambda}\left(\frac{1}{r^2} - \frac{\lambda'}{r}\right), \tag{2.27}$$

$$8\pi G\, T_0^{\ r} = -e^{-\lambda}\frac{\dot{\lambda}}{r}, \tag{2.28}$$

$$8\pi G\, T_r^{\ r} = \frac{1}{r^2} - e^{-\lambda}\left(\frac{\nu'}{r} + \frac{1}{r^2}\right), \tag{2.29}$$

$$\begin{aligned}
8\pi G\, T_\theta^{\ \theta} = 8\pi G\, T_\phi^{\ \phi} &= \frac{1}{2}e^{-\nu}\left(\ddot{\lambda} + \frac{\dot{\lambda}^2}{2} - \frac{\dot{\lambda}\dot{\nu}}{2}\right) \\
&- \frac{1}{2}e^{-\lambda}\left(\nu'' + \frac{\nu'^{\,2}}{2} + \frac{\nu' - \lambda'}{r} - \frac{\nu'\lambda'}{2}\right).
\end{aligned} \tag{2.30}$$

The function $\lambda(r,t)$ is chosen to be defined in the Schwarzschild sense,

$$e^{\lambda} = \left(1 - \frac{2GM}{r}\right)^{-1}, \tag{2.31}$$

however in this case, it is made time-dependent through the fact that the enclosed mass $M = M(r,t)$ is a function of time t. Applying the fact that

$$e^{-\lambda}\lambda' = e^{-\lambda}\frac{d\lambda}{dr} = \frac{2GM'}{r} - \frac{2GM}{r^2},$$

to eq. (2.27) gives

$$\frac{dM}{dr} = 4\pi r^2 T_0{}^0. \tag{2.32}$$

Similarly, considering that

$$e^{-\lambda}\dot{\lambda} = e^{-\lambda}\frac{d\lambda}{dt} = \frac{2G\dot{M}}{r},$$

eq. (2.28) becomes

$$\frac{dM}{dt} = -4\pi r^2 T_0{}^r. \tag{2.33}$$

Substituting $e^{-\lambda}$ and rearranging eq. (2.29) gives the function $\nu(r,t)$ in a first order differential equation

$$\frac{\nu'}{2} = \frac{1}{2}\frac{d\nu}{dr} = \frac{G}{r}\left(\frac{M - 4\pi r^3 T_r{}^r}{r - 2GM}\right). \tag{2.34}$$

Considering the commutation of the ordinary derivatives $\frac{d}{dr}\dot{M} = \frac{d}{dt}M'$ and using Eqs. (2.32) and (2.33), the following becomes evident,

$$\dot{T}_0{}^0 + \frac{1}{r^2}\left(r^2 T_0{}^r\right)' = 0. \tag{2.35}$$

This can also be shown by considering the continuity equation

$$T_\mu{}^\nu{}_{;\nu} = 0, \tag{2.36}$$

which, for the index $\mu = 0$ and using the covariant derivative $T_\mu{}^\nu{}_{;\nu} = \partial_\nu T_\mu{}^\nu + \Gamma^\nu_{\alpha\nu} T_\mu{}^\alpha - \Gamma^\alpha_{\mu\nu} T_\alpha{}^\nu$, becomes

$$\dot{T}_0{}^0 + \frac{1}{r^2}\left(r^2 T_0{}^r\right)' = -\frac{1}{2}\left[\dot{\lambda}\left(T_0{}^0 - T_r{}^r\right) + \left(\nu' + \lambda'\right) T_0{}^r\right]. \tag{2.37}$$

Now by subtracting the first and third of the Einstein field equations like Eqs. (2.27) - (2.29) gives

$$8\pi G\,\left(T_0{}^0 - T_r{}^r\right) = \frac{e^{-\lambda}}{r}\left(\nu' + \lambda'\right), \tag{2.38}$$

and using Eq. (2.28) shows that

$$\dot{\lambda}\left(T_0^{\ 0} - T_r^{\ r}\right) = -\left(\nu' + \lambda'\right) T_0^{\ r}, \tag{2.39}$$

which means that the right hand side of Eq. (2.37) vanishes. Furthermore, the continuity relation Eq. (2.36) for the index $\mu = r$ gives

$$\dot{T}_r^{\ 0} + \frac{\dot{\nu} + \dot{\lambda}}{2} T_r^{\ 0} + \frac{1}{r^2}\left(r^2 T_r^{\ r}\right)' = \frac{\nu'}{2}\left(T_0^{\ 0} - T_r^{\ r}\right) + \frac{1}{r}\left(T_\theta^{\ \theta} + T_\phi^{\ \phi}\right), \tag{2.40}$$

which is analogous to the Euler equation in fluid dynamics. Having extracted useful results from the set of Einstein field equations Eqs. (2.27), (2.28) and (2.29), the remaining Eq. (2.30) yields only identities and hence no further information.

2.4 Specifying the matter content

To summarize, the set of equations to describe the accretion flow is

$$\frac{dM}{dr} = 4\pi r^2 T_0^{\ 0}, \tag{2.41}$$

$$\frac{dM}{dt} = -4\pi r^2 T_0^{\ r}, \tag{2.42}$$

$$\frac{1}{2}\frac{d\nu}{dr} = \frac{G}{r}\left(\frac{M - 4\pi r^3 T_r^{\ r}}{r - 2GM}\right). \tag{2.43}$$

As these equations are still very general, a specific matter content is yet to be imposed. This is done by choosing the energy-momentum tensor for a perfect fluid,

$$T_\mu^{\ \nu} = (\rho + P)\, U_\mu U^\nu - \delta_\mu^{\ \nu} P. \tag{2.44}$$

It must be stipulated that this will be a model of stationary accretion flow, such that $\dot{\rho} = \dot{P} = 0$ and that the flow of matter through any spherical shell around the origin is the same. This implies that $\left(\dot{M}\right)' = 0$. Following this line of reasoning, $(r^2 T_0^{\ r})' = 0$ and considering Eq. (2.35) this means that $\dot{T}_0^{\ 0} = 0$ as well. From this it becomes clear that the 4-velocity obeys the relation $\frac{d}{dt} U_0 U^0 = 0$ and from the fact that $U_\mu U^\mu = 1$, this

requires that $\frac{d}{dt}U_r U^r = 0$, also. This leads to the introduction of a new flow velocity v to parameterise the four-velocity U^μ, such that

$$U^0 = \frac{e^{-\nu/2}}{\sqrt{1-v^2}}, \qquad U^r = -\frac{v e^{-\lambda/2}}{\sqrt{1-v^2}}. \tag{2.45}$$

where $\dot{v} = 0$ is a direct consequence of the stationary model. Now write the energy-momentum tensor in terms of the new flow velocity v like

$$\begin{aligned}
T_0^{\ 0} &= (\rho + P)\, U_0 U^0 - P = \frac{\rho + P}{1-v^2} - P = \frac{\rho + v^2 P}{1-v^2}, && (2.46)\\
T_0^{\ r} &= (\rho + P)\, U_0 U^r = -(\rho + P)\, \frac{v}{1-v^2}\, e^{\frac{\nu-\lambda}{2}}, && (2.47)\\
T_r^{\ r} &= -(\rho + P)\, U_r U^r - P = -(\rho + P)\, \frac{v^2}{1-v^2} - P = -\frac{P + v^2\rho}{1-v^2}, && (2.48)\\
T_\theta^{\ \theta} &= T_\phi^{\ \phi} = -P. && (2.49)
\end{aligned}$$

Applying these specifications and Eq. (2.31) to Eq. (2.41),(2.42) and (2.43) gives

$$\begin{aligned}
\frac{dM}{dr} &= 4\pi r^2 \left(\frac{\rho + v^2 P}{1-v^2}\right), && (2.50)\\
\frac{dM}{dt} &= 4\pi r^2 (\rho + P)\, \frac{v}{1-v^2} \sqrt{1 - \frac{2GM}{r}}\, e^{\nu/2}, && (2.51)\\
\frac{1}{2}\frac{d\nu}{dr} &= \frac{1}{1-v^2}\frac{G}{r}\left[\frac{M(1-v^2) + 4\pi r^3 (P + v^2\rho)}{r - 2GM}\right], && (2.52)
\end{aligned}$$

where $\nu/2$ can be interpreted as a general relativistic analogue of the Newtonian potential. Next, recall the generalised Euler equation for fluid flow Eq. (2.40), working out the individual parts as follows. Starting with Eq. (2.47) and differentiating with respect to time

$$\dot{T}_r^{\ 0} + \frac{\dot{\nu} + \dot{\lambda}}{2} T_r^{\ 0} = \dot{\lambda} e^{\frac{\lambda-\nu}{2}} \frac{(\rho + P)\, v}{1-v^2}. \tag{2.53}$$

The next term is worked out by considering the stationary flow condition that $\left(\dot{M}\right)' = 0$ and applying this to Eq. (2.51) yields the relation

$$\frac{1}{r^2}\left[r^2 \frac{(\rho + P)\, v}{1-v^2}\right]' = -\frac{\nu' - \lambda'}{2} \frac{(\rho + P)\, v}{1-v^2}. \tag{2.54}$$

Now taking the energy-momentum tensor component from Eq. (2.48)

$$\begin{aligned}
\frac{1}{r^2}\left(r^2 T_r^{\ r}\right)' &= -\frac{1}{r^2}\left[r^2 \frac{(\rho + P)\, v}{1-v^2}\right]' v - \frac{(\rho + P)\, v}{1-v^2} v' - \frac{2P}{r} - P'\\
&= \frac{\nu' - \lambda'}{2} \frac{(\rho + P)\, v^2}{1-v^2} - \frac{(\rho + P)\, v}{1-v^2} v' - \frac{2P}{r} - P'. && (2.55)
\end{aligned}$$

From Eq. (2.46) and (2.48), find that

$$T_0{}^0 - T_r{}^r = (\rho + P)\,\frac{1+v^2}{1-v^2}. \tag{2.56}$$

So now, using Eqs. (2.53), (2.55), (2.56) and (2.49) in Eq. (2.40) a result relating the radial derivatives of the flow velocity v, the proper pressure P and metric function ν is found

$$vv' + \left(1-v^2\right)\frac{P'}{\rho+P} + \frac{\nu'}{2} - \dot{\lambda}e^{\frac{\lambda-\nu}{2}}v + \frac{\lambda'}{2}v^2 = 0 \tag{2.57}$$

To find the terms involving λ' and $\dot{\lambda}$ in the previous equation, consider Eqs. (2.27) and (2.28)

$$\frac{\lambda'}{2}v^2 = \left[4\pi G r\left(\frac{\rho+P}{1-v^2} - P\right) - \frac{GM}{r^2}\right]v^2 e^{\lambda}, \tag{2.58}$$

$$\dot{\lambda}e^{\frac{\lambda-\nu}{2}}v = 8\pi G r\left(\frac{\rho+P}{1-v^2}\right)v^2 e^{\lambda}. \tag{2.59}$$

Therefore, the combination of the two terms is

$$-\dot{\lambda}e^{\frac{\lambda-\nu}{2}}v + \frac{\lambda'}{2}v^2 = -\frac{G}{r^2}e^{\lambda}\left\{Mv^2 + 4\pi r^3\left[\frac{(\rho+P)v^2}{1-v^2} + Pv^2\right]\right\}. \tag{2.60}$$

Taking the result of $\nu'/2$ from Eq. (2.43) and combining with the previous result gives

$$\frac{\nu'}{2} - \dot{\lambda}e^{\frac{\lambda-\nu}{2}}v + \frac{\lambda'}{2}v^2 = \left(1-v^2\right)\frac{G}{r^2}e^{\lambda}\left(M + 4\pi r^3 P\right) \tag{2.61}$$

Thus the generalised version of the Tolman-Oppenheimer-Volkoff (TOV) equations [34, 31] is derived to be

$$\frac{vv'}{1-v^2} + \frac{P'}{\rho+P} + \frac{G}{r}\left(\frac{M+4\pi r^3 P}{r-2GM}\right) = 0. \tag{2.62}$$

This relation reduces to the original TOV equation when the flow velocity vanishes and the system's flow becomes static.

2.5 Separating the generalised TOV equation

The TOV equation is a direct result of energy conservation in the system and Eq. (2.62) gives us one relation involving the radial derivatives of the flow velocity v and the pressure of the fluid P. To perform any meaningful analysis on the accretion problem, two

distinct equations for the respective derivatives would need to be known. To separate the equation, consider again that $\left(\dot{M}\right)' = 0$ by differentiating Eq. (2.51),

$$\frac{2}{r} + \frac{\rho' + P'}{\rho + P} + \frac{v'}{v} + \frac{2vv'}{1-v^2} + \frac{\nu'}{2} + \frac{Gr}{r - 2GM}\left(\frac{M}{r^2} - \frac{M'}{r}\right) = 0 \tag{2.63}$$

The radial derivatives of M and ν are already known through Eq. (2.50) and Eq. (2.52) respectively, so Eq. (2.63) becomes

$$\begin{aligned}\frac{2}{r} + \frac{\rho'}{\rho + P} + \frac{P'}{\rho + P} \quad &+ \quad \frac{v'}{v\left(1-v^2\right)} + \frac{vv'}{1-v^2} + \frac{G}{r\left(r-2GM\right)}\left[M + 4\pi r^3\left(\frac{P + v^2\rho}{1-v^2}\right)\right] \\ &+ \quad \frac{G}{r\left(r-2GM\right)}\left[M - 4\pi r^3\left(\frac{\rho + v^2 P}{1-v^2}\right)\right] = 0\end{aligned} \tag{2.64}$$

Rearranging this gives a more recognisable relation, namely

$$\begin{aligned}\frac{2}{r} + \frac{\rho'}{\rho + P} + \frac{v'}{v\left(1-v^2\right)} \quad &+ \quad \frac{G}{r}\left(\frac{M - 4\pi r^3\rho}{r - 2GM}\right) \\ + \frac{P'}{\rho + P} + \frac{vv'}{1-v^2} \quad &+ \quad \frac{G}{r}\left(\frac{M + 4\pi r^3 P}{r - 2GM}\right) = 0.\end{aligned} \tag{2.65}$$

The lower half of Eq. (2.65) vanishes, as it is identical to the TOV relation Eq. (2.62). That leaves

$$\frac{2}{r} + \frac{\rho'}{\rho + P} + \frac{v'}{v\left(1-v^2\right)} + \frac{G}{r}\left(\frac{M - 4\pi r^3\rho}{r - 2GM}\right) = 0. \tag{2.66}$$

Performing the manipulation of multiplying Eq. (2.66) by v^2 and subtracting it from Eq. (2.62) results in a first order equation for ρ as given by

$$\frac{c_S^2 - v^2}{\rho + P}\rho' + \frac{G}{r}\left[\frac{M(1-v^2) + 4\pi r^3(P + v^2\rho)}{r - 2GM}\right] - \frac{2v^2}{r} = 0, \tag{2.67}$$

where the speed of sound of the fluid $c_S^2 = \frac{dP}{d\rho}$ is introduced. Using this equation it is possible to calculate a similar relation for the radial derivative of the flow speed v such that

$$\frac{c_S^2 - v^2}{1-v^2}\frac{v'}{v} - \frac{G}{r}\left[\frac{M(1-c_S^2) + 4\pi r^3(P + c_S^2\rho)}{r - 2GM}\right] + \frac{2c_S^2}{r} = 0. \tag{2.68}$$

Thus by combining the generalised TOV relation Eq. (2.62) and the stationary flow constraint $\left(\dot{M}\right)' = 0$, two first order equations are produced for the fluid density ρ and

the flow velocity v,

$$\frac{c_S^2 - v^2}{\rho + P}\frac{d\rho}{dr} = \frac{2v^2}{r} - \frac{G}{r}\frac{M\left(1-v^2\right) + 4\pi r^3\left(P + v^2\rho\right)}{r - 2GM}, \tag{2.69}$$

$$\frac{c_S^2 - v^2}{1 - v^2}\frac{1}{v}\frac{dv}{dr} = \frac{G}{r}\frac{M\left(1-c_S^2\right) + 4\pi r^3\left(P + c_s^2\rho\right)}{r - 2GM} - \frac{2c_S^2}{r}. \tag{2.70}$$

Eqs. (2.50), (2.69) and (2.70) completely describe the radial stationary accretion flow in a system of first-order equations. Thus the highly nonlinear system is solvable using numerical methods such as a variable-step Runge-Kutta method.

Comparison with the Bondi accretion formalism is made by inspecting the mass accretion formula given by Eq. (2.51). The new accretion equation differs by a factor of the metric functions λ and ν. This factor shall be introduced as a reduced potential $\psi/2$, such that

$$e^{\psi/2} = e^{(\nu+\lambda)/2} = \left(1 - \frac{2GM}{r}\right)^{-1/2} e^{\nu/2}, \tag{2.71}$$

where the new function can be found by the relation

$$\frac{1}{2}\,\frac{d\psi}{dr} = 4\pi G r^2 \left(\frac{1+v^2}{1-v^2}\right)\frac{(\rho + P)}{r - 2GM}. \tag{2.72}$$

This value of $\psi/2$ can quantify the departure from the Bondi approximation of the accretion process.

Chapter 3

Test Cases of the relativistic accretion theory

3.1 Stiff matter and radiation accreted relativistically

A suitable test case for the treatment of relativistic accretion is to consider a simplified version of a relativistic system, such as the model of a polytropic equation of state, i.e.

$$P = \kappa n^{\Gamma}. \tag{3.1}$$

Utilising the total energy density $\rho = mn + \epsilon'$, where ϵ' is the internal energy, applying mass-energy conservation and finally integrating this becomes [6]

$$P = (\Gamma - 1)(\rho - mn), \tag{3.2}$$

after eliminating the number density n. This equation of state approximates ultrarelativistic matter, i.e. with particle mass m set to 0, and relates the pressure proportionally to the mass density, $P = w\rho$, where the parameter $w = c_S^2$ represents the square of the speed of sound in the accreting material and is related to the polytropic index Γ. This particularly simple equation of state allows an easy test for the relativistic accretion model as there exist analytical solutions for special values of the parameter w;

namely $w = 1$ and $w = 1/3$. The system of relativistic accretion equations, comprised of Eqs. (2.50), (2.69) and (2.70), then becomes

$$\frac{dM}{dr} = 4\pi r^2 \rho \left(\frac{1 + w v^2}{1 - v^2} \right), \tag{3.3}$$

$$\frac{d\rho}{dr} = \frac{\rho}{r} \left(\frac{1 + w}{w - v^2} \right) \left[2v^2 - G \frac{M\left(1 - v^2\right) + 4\pi r^3 \rho \left(w + v^2\right)}{r - 2GM} \right], \tag{3.4}$$

$$\frac{dv}{dr} = \frac{v}{r} \left(\frac{1 - v^2}{w - v^2} \right) \left[G \frac{M\left(1 - w\right) + 4\pi r^3 \rho \left(2w\right)}{r - 2GM} - 2w \right]. \tag{3.5}$$

3.1.1 Stiff matter accretion results

Firstly, for the case of relativistic stiff matter, the speed of sound becomes the speed of light, such that $w = 1$. This is an unphysical case, as it violates causality and is usually not applied to particles but fields rather. It, however, serves the purpose of testing the numerical code against the analytical solutions mentioned above. It must be stipulated that this analytical solution brought by Babichev *et al* [7] can only test the numerical code describing the relativistic accretion theory in the limit of a "test-fluid" of negligible mass being accreted by a dominating central object, the same simplifying assumption made by Bondi and later Michel.

Making predictions about the flow, it is expected that the accretion of stiff matter should not yield transonic flow, as the speed of sound is equivalent to the speed of light and is hence the bounding limit of the fluid flow. This means that a smooth flow of the accretion material toward the center is expected in the stationary model. The analytical solutions for the density and velocity functions, taken from [7], are given by Eqs. (2.16) and (2.17). In these equations the radial flow velocity $U(r)$ is related to the already-defined velocity parameter $v(r)$ through Eqs. (2.45). Numeric solutions to the relativistic accretion equations of stiff matter are depicted in Figs. 3.1 and 3.2 and the analytical solutions for test fluid accretion are shown along side for comparison.

3.1.2 Radiation accretion results

In the second case that allows analytical solutions, the case of radiation accretion, the equation of state parameter w is set to $1/3$. this in turn is a physical case for an equation of state. Again, the analytical solutions are only valid for the "test-fluid" limit and serve to test the numerical code for consistency.

The theoretical analysis of Michel [5] predicts that there be a critical point in the flow at $r_c = 3GM$. At this particular point, the flow velocity of the fluid will reach the speed of sound of the accreting material. In the case when the fluid reaches the speed of sound at a radius larger than that given by the critical point for the analytical solution (red-dotted line in Fig. 3.4), a departure from the smooth fluid flow is expected. This would come about in systems that are overly dense at the boundary, causing an accelerated infall of matter compared to the case of a smooth transition through the critical point as is observed in the analytical solution. As with objects such as planes moving through the earth's atmosphere approaching the sound barrier and producing a sonic boom, a shock phenomenon in the fluid flow is expected for such cases. The analytical solutions for the density profile in this case becomes somewhat more complicated, again taken from [7], and is given by Eqs. (2.18). From this the flow velocity function can be calculated numerically. The solutions to the system of equations for various densities at the boundary are laid out below along with the relevant analytical solutions [7].

Working out the numerical value of the accretion rate given by Eq. (2.51) for several values of $m_H = 1 - \frac{M_c}{M}$ the mass of the halo surrounding the central object, the accretion profile curve is generated and plotted below. This can be compared with work done by Malec *et al* [9, 10], in which the accretion rate is calculated for polytropic equations of state including the feature of backreaction. Since the halo mass m_H is shown to be proportional to the energy density at the boundary ρ_∞ and the accretion rate $\dot{M} \propto \rho_\infty M^2$, we can rearrange this and find that

$$\dot{M} \propto m_H \left(1 - m_H\right)^2, \tag{3.6}$$

which is a good fit for the accretion rate curve produced by the model. Some scatter is

observed in the data, especially around the peak of the curve. This can be explained by slight numerical errors that enter into the calculations when the fluid flow features the observed instability or shock, in the vicinity of the critical point of $r_c = 3GM$, as seen in Fig (3.4).

3.1.3 Discussion of test results

The tests conducted on the relativistic accretion theory in the above section have shown reasonable, understandable results for the simple fluids that they model. Furthermore, the results meet the analytical solutions of the test-fluid cases with very good agreement, as can be seen with the flow velocity curve in Fig. 3.3. This lends the theory increased credibility in its resulting numerical solutions and confidence in its predictive power.

The relation between the density at the observer ρ_∞ and the central accreting object's mass m_C, depicted in Fig. 3.5, are consistent with results published by Malec *et al* [9, 10]. The accretion rate curve in Fig. 3.6 shows the quenching of the accretion process for the regimes of dominating accreting fluid around a small central condensed object and the opposite limit, the test-fluid scenario. This also agrees well with work done by Malec *et al* [9, 10], as Eq. (3.6) is a good fit for the numerical results calculated from the relativistic accretion theory.

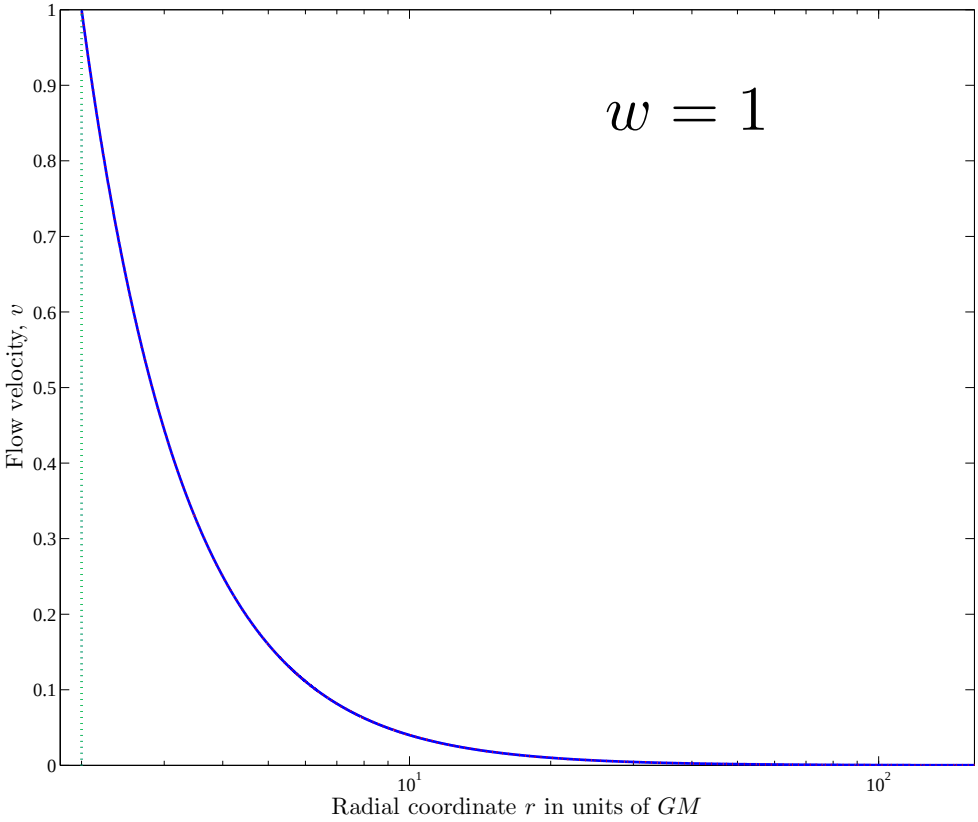

Figure 3.1: The fluid flow velocity v for the relativistic stiff matter equation of state agrees well with the analytical solution. The profile does not vary with for various values of the halo mass m_H.

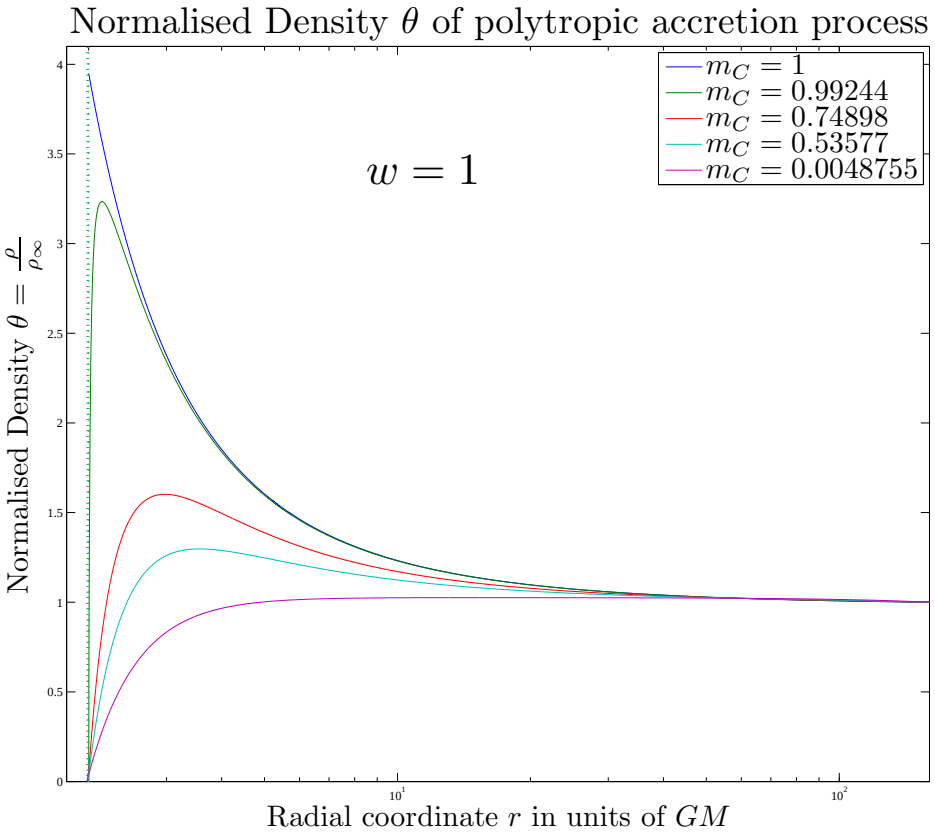

Figure 3.2: A depiction of the density profiles for various central mass ratios in the case of the toy model of ultrarelativistic stiff matter, where $w = 1$. The numerical solution for the test-fluid case of $m_C = M$ agrees with the analytical solution in [7] with negligible error.

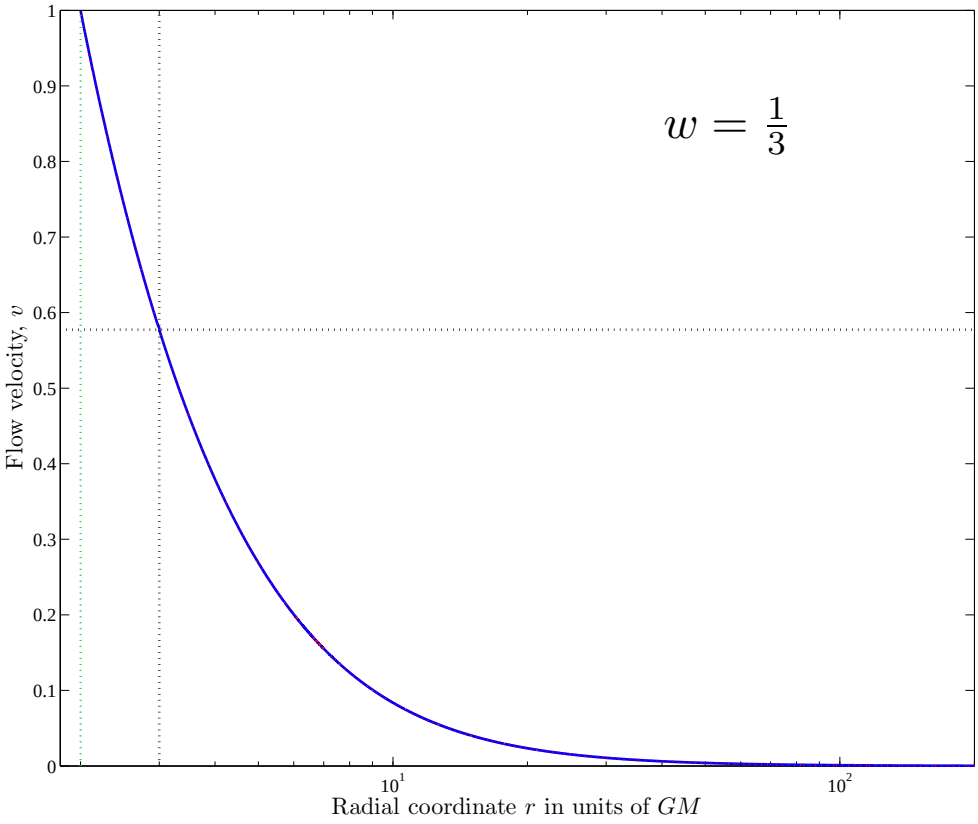

Figure 3.3: For the test-fluid case of negligible halo mass m_H, the accretion flow is smooth and agrees well with the analytical solution. Here the horizontal dotted line represents the speed of sound in the fluid, i.e. $\sqrt{w}$, and the vertical dotted line shows the critical point for the analytical solution for radiation flow from the solutions by Babichev *et al.*

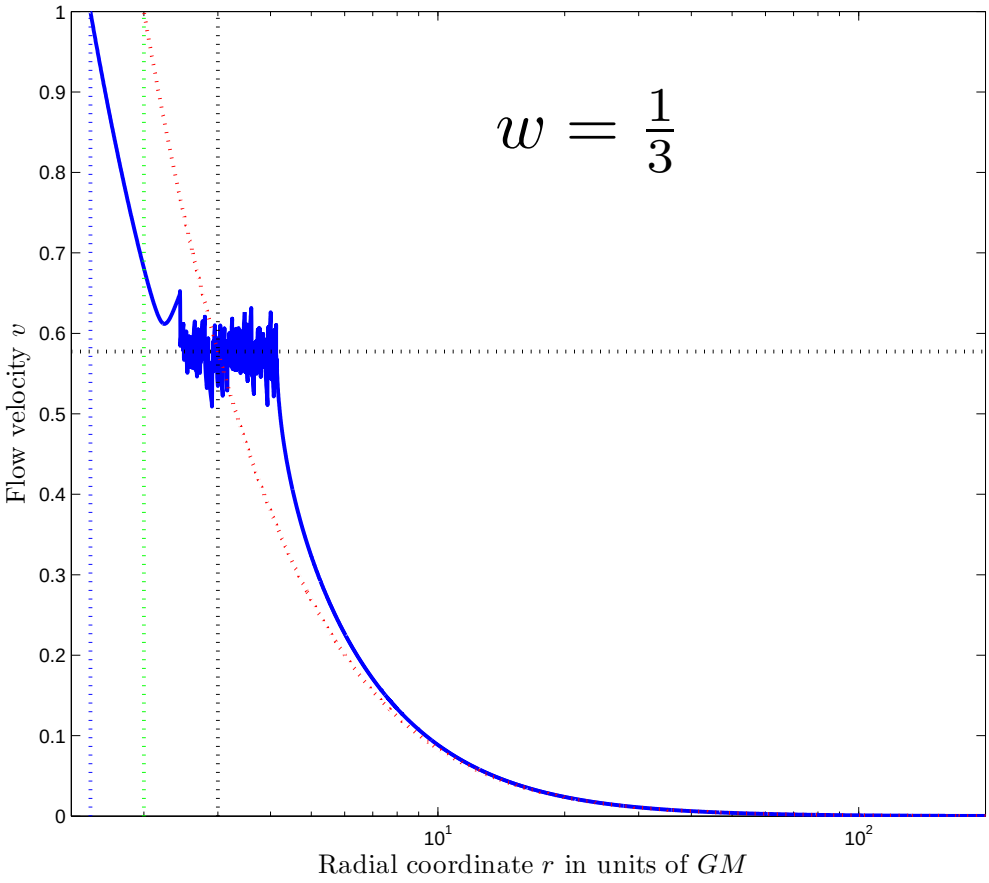

Figure 3.4: In the case of comparable mass between halo and central accreting object, the flow exhibits shock as the fluid flow reaches the speed of sound ahead of the point where the analytical solution (red-dotten curve) reaches its critical point. The ratio of m_H/M for this figure is 0.2537. Here the black horizontal dotted line represents the speed of sound in the fluid, i.e. $\sqrt{w}$, and the black vertical dotted line shows the critical point for the analytical solution for radiation flow from the solutions by Babichev *et al.* The other vertical lines represent the apparent horizons of the central accreting object: green for the analytical solution, blue for the calculated case.

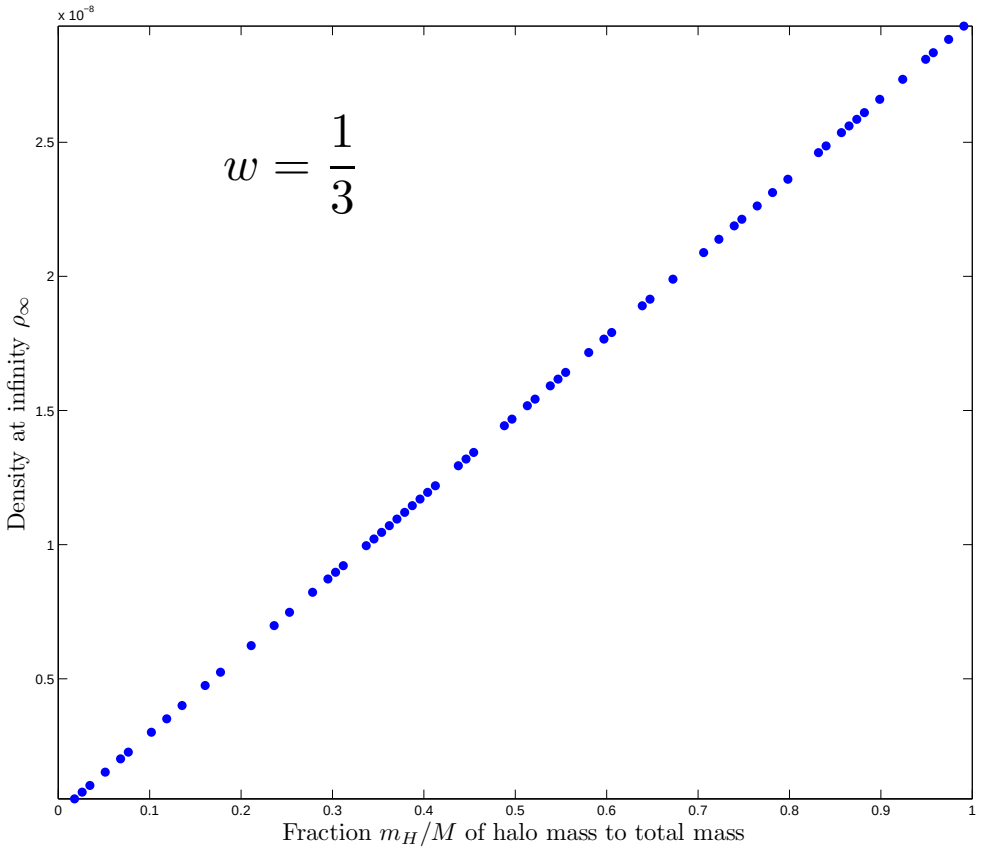

Figure 3.5: The relativistic accretion model reproduces a proportionality between the boundary density value and the resulting halo mass, in agreement with Malec *et al* [9, 10].

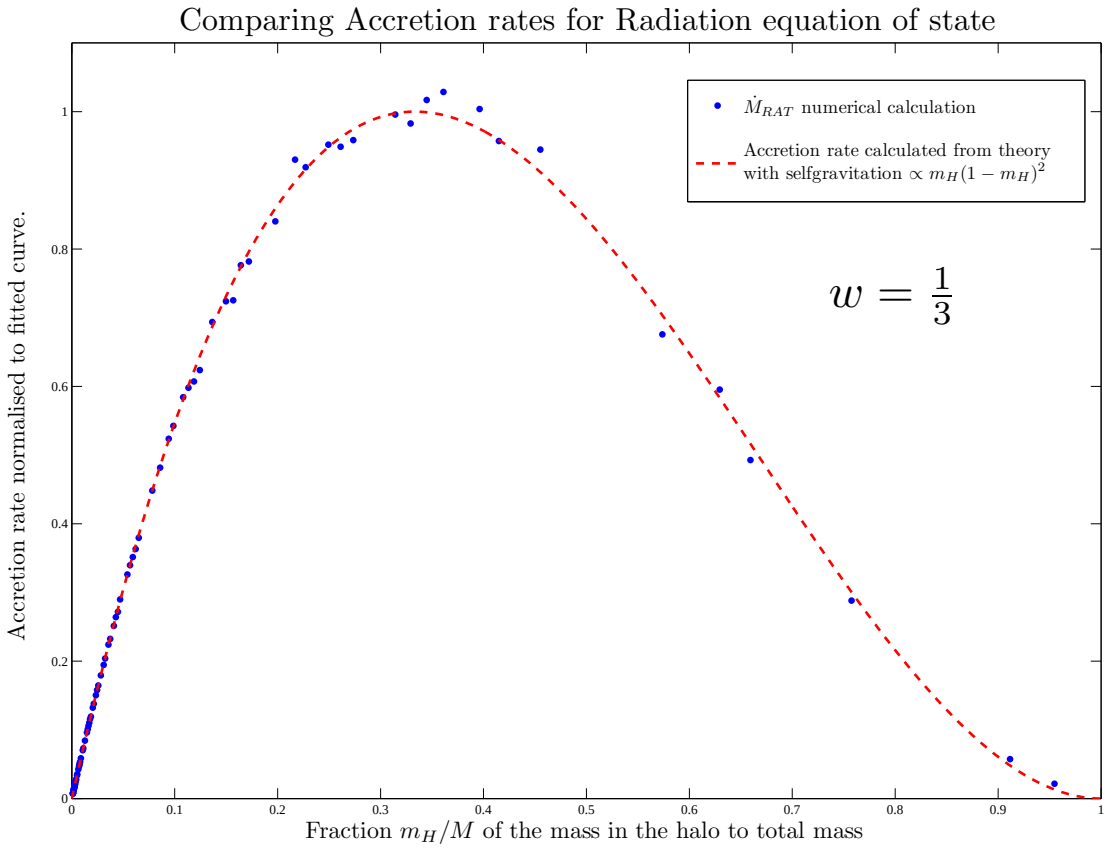

Figure 3.6: The accretion rates calculated by the numerical model (points) for values of $0 \leqslant m_H \leqslant 1$ show good agreement with the curve set forth by Malec *et al* [9, 10] (dashed), with the scatter around the peak of the curve due to numerical features caused by shock exhibited in the fluid flow.

Chapter 4

Results for the accretion of a relativistic Fermi gas

The symbiotic scenario described in [12] relies on the idea that SMBHs grew rapidly in the early universe due to an abundance of supermassive dark matter sterile neutrino balls, which they accreted in an Eddington limit-less process. Thus it would be prudent to use this new relativistic accretion theory to model the growth of a central body feeding on a surrounding fluid comprised of a relativistic Fermi gas.

4.1 Relativistic accretion of a degenerate relativistic Fermi gas

To model the accretion of a degenerate Fermi gas, as would be needed to describe dark matter in the form of degenerate sterile neutrinos falling into a central black hole, an appropriate equation of state must be utilised. The equation of state for a degenerate ideal Fermi gas, taken from [6], has the parameterization for the pressure P and the energy density ρ

$$P(X) = k\left\{X\left(1+X^2\right)^{1/2}\left(2X^2/3-1\right)+\ln\left[X+\left(1+X^2\right)^{1/2}\right]\right\}, \qquad (4.1)$$

$$\rho(X) = \frac{k}{c^2}\left\{X\left(1+X^2\right)^{1/2}\left(2X^2+1\right)-\ln\left[X+\left(1+X^2\right)^{1/2}\right]\right\}, \tag{4.2}$$

where X is the dimensionless Fermi momentum

$$X = \frac{p_F}{m_\nu c}, \tag{4.3}$$

and the mass of the fermion is represented by m_ν. The constant k is given by

$$k = \frac{g_\nu m_\nu^4 c^5}{16\pi^2\hbar^3} = \frac{m_\nu c^2}{\lambda_\nu^3}, \tag{4.4}$$

where $\lambda_\nu = h/(m_\nu c)$ is the Compton wavelength of the fermion and g_ν is its degeneracy factor. In this situation, the speed of sound of the fluid is given by

$$c_S^2 = \frac{\partial P}{\partial \rho} = \frac{1}{3}\frac{X^2}{1+X^2}. \tag{4.5}$$

Expanding the following expressions

$$\frac{P(X)+v^2\rho(X)}{1-v^2} = P(X)+\alpha(X,v) = \tilde{P}(X,v), \tag{4.6}$$

$$\frac{\rho(X)+v^2P(X)}{1-v^2} = \rho(X)+\alpha(X,v) = \tilde{\rho}(X,v), \tag{4.7}$$

where $\alpha(X,v) = [P(X)+\rho(X)]\,\frac{v^2}{1-v^2} = \frac{8}{3}\,kX^3(1+X^2)^{1/2}\frac{v^2}{1-v^2}$, the relativistic accretion theory generates the following system of equations

$$\frac{dM}{dr} = 4\pi r^2\tilde{\rho}(X,v), \tag{4.8}$$

$$\frac{3}{X}\frac{dX}{dr} = \frac{1}{r\left(c_S^2-v^2\right)}\left\{2v^2-\frac{G\left(1-v^2\right)}{r-2GM}\left[M+4\pi r^3\tilde{P}(X,v)\right]\right\}, \tag{4.9}$$

$$\frac{1}{v}\frac{dv}{dr} = \frac{1-v^2}{r\left(c_S^2-v^2\right)}\left\{\frac{G\left(1-c_S^2\right)}{r-2GM}\left[M+4\pi r^3\tilde{P}(X,c_S)\right]-2c_S^2\right\}. \tag{4.10}$$

Similarly, the mass accretion rate and the analogue of the Newtonian potential can be expressed in terms of this parameter X, such that

$$\frac{dM}{dt} = 4\pi r^2\left[\frac{8}{3}\,kX^3(1+X^2)^{1/2}\frac{v}{1-v^2}\right]\sqrt{1-\frac{2GM}{r}}e^{\nu/2}, \tag{4.11}$$

$$\frac{1}{2}\frac{d\nu}{dr} = \frac{G}{r}\left[\frac{M+4\pi r^3\tilde{P}(X,v)}{r-2GM}\right], \tag{4.12}$$

or rather, working with the function $\psi/2$

$$\frac{1}{2}\frac{d\psi}{dr} = 4\pi G r^2 \left(\frac{1+v^2}{1-v^2}\right)\frac{\rho+P}{r-2GM} \tag{4.13}$$

Again, the numerical solution is calculated by integrating the system of equations Eqs. (4.8)-(4.10) from some outer boundary, simulated to be infinity, toward the central accreting object. Now the density at the outer boundary used in previous numerical integrations, ρ_∞, will be replaced by the non-dimensional Fermi momentum at the outer boundary, x_∞.

4.1.1 Non-dimensionalisation

At this point it is prudent to introduce a dimensional scale for the mass and radius in the model in order to non-dimensionalise the equations of relativistic accretion for the relativistic Fermi gas. As in [32], let $r = a_\nu x$ and $M = b_\nu \mu$ where

$$a_\nu = 2\sqrt{\frac{\pi}{g_\nu}}\left(\frac{m_P}{m_\nu}\right)^2 l_P = 2.6839\times 10^{10}\left(\frac{15\text{ keV}}{m_\nu c^2}\right)\left(\frac{2}{g_\nu}\right)^{1/2}\text{ km}, \tag{4.14}$$

$$b_\nu = 2\sqrt{\frac{\pi}{g_\nu}}\left(\frac{m_P}{m_\nu}\right)^2 m_P = 1.8172\times 10^{10} M_\odot\left(\frac{15\text{ keV}}{m_\nu c^2}\right)\left(\frac{2}{g_\nu}\right)^{1/2}. \tag{4.15}$$

where $m_P = (\hbar c/G)^{1/2}$ and $l_P = (\hbar G/c^3)^{1/2}$ are the Planck mass and length respectively. The OV-limit mentioned earlier is given by $\mu_{OV} = 0.15288$ in units of b_ν. Introducing these dimensionless quantities to the relativistic accretion model, $P(X) \to \phi(X) = P(X)/k$ and $\rho(X) \to \chi(X) = c^2\rho(X)/k$ and the system of Eqs. (4.8) - (4.10) become

$$\frac{d\mu}{dx} = x^2\tilde{\chi}(X,v), \tag{4.16}$$

$$\frac{3}{X}\frac{dX}{dx} = \frac{1}{x\left(c_S^2-v^2\right)}\left\{2v^2 - \frac{(1-v^2)}{x-2\mu}\left[\mu + x^3\tilde{\phi}(X,v)\right]\right\}, \tag{4.17}$$

$$\frac{1}{v}\frac{dv}{dx} = \frac{1-v^2}{x\left(c_S^2-v^2\right)}\left\{\frac{(1-c_S^2)}{x-2\mu}\left[\mu + x^3\tilde{\phi}(X,c_S)\right] - 2c_S^2\right\}. \tag{4.18}$$

A time scale will need to be introduced to rewrite the mass accretion equation in non-dimensional form, such that $t = c_\nu\tau$ and

$$\frac{d\mu}{d\tau} = x^2X^3\left(1+X^2\right)^{1/2}\frac{v}{1-v^2}\left(1-\frac{2\mu}{x}\right)e^{\psi/2}, \tag{4.19}$$

where

$$c_\nu = \frac{3}{4}\sqrt{\frac{\pi}{g_\nu}}\left(\frac{m_P}{m_\nu}\right)^2 ct_P = 0.31915\left(\frac{15\text{ keV}}{m_\nu c^2}\right)\left(\frac{2}{g_\nu}\right)^{1/2}\text{ Myr.} \tag{4.20}$$

Here, $t_P = (\hbar G/c^5)^{1/2}$ is the Planck time. Conversely, the mass accretion equation has units of

$$\gamma_\nu = \frac{b_\nu}{c_\nu} = \frac{8}{3}\frac{c^2}{G} = 5.6937 \times 10^4 M_\odot \text{ yr}^{-1}. \tag{4.21}$$

4.2 Discussion of numerical results

The non-dimensionalisation of the previous section defined the scales of mass and length of the system. In the treatment of such large systems of fermions, the OV-limit sets an upper bound on the total mass and thus the boundary conditions set in the numerical integration must reflect this. The first result case will be for a value of $\mu_\infty = 5 \times 10^{-4}$, equivalent to a mass of $9.0843 \times 10^6 M_\odot$, roughly 0.3% of the OV-limit.

The numerical solution to the relativistic accretion equations for a relativistic Fermi gas yielded flow velocity profiles as seen in Figs. 4.1, 4.2 and 4.3. These figures show many similarities to the case of accretion of a polytropic fluid with $w = 1/3$; the initial monotonic increase of the flow velocity until the speed of sound c_S is reached, then an oscillation of the flow speed about the speed of sound as is akin to a shock-like flow and then the eventual monotonic increase toward c at the horizon of the central object. With this equation of state for relativistic fermions, however, the speed of sound c_S is itself changing throughout the region of integration. At first, as the flow speed increases, the sound speed remains roughly constant until the two values meet and both then become jagged functions. Through out the region where both flow velocity and sound speed are non-smooth, they are both still increasing. Once the flow v becomes smooth again the same is true for c_S and it increases toward its maximal value, which is equal to $1/\sqrt{3}$ for the case of small central mass m_C and less than that for cases closer to the test-fluid scenario.

Looking at a range of boundary conditions that result in solutions with central mass in the range $0 < m_C < 1$, there are further comparisons that can be made to

the polytropic case. The relation between the boundary condition of density ρ_∞ is directly proportional to the mass of the halo of fluid surrounding the central body, seen in Fig. 4.4, just as it was in the accretion of radiation in the test case.

The accretion rate picture shown in Fig. 4.5 shows less similarity than the test case. Only for the test-fluid regime is the accretion rate quenched. It then peaks for a value of $m_H = 0.4109$ and then stays roughly constant. The numerical data from the Fermi gas case look a lot more like the accretion shut-off function calculated from the Newtonian model of the symbiotic scenario [12].

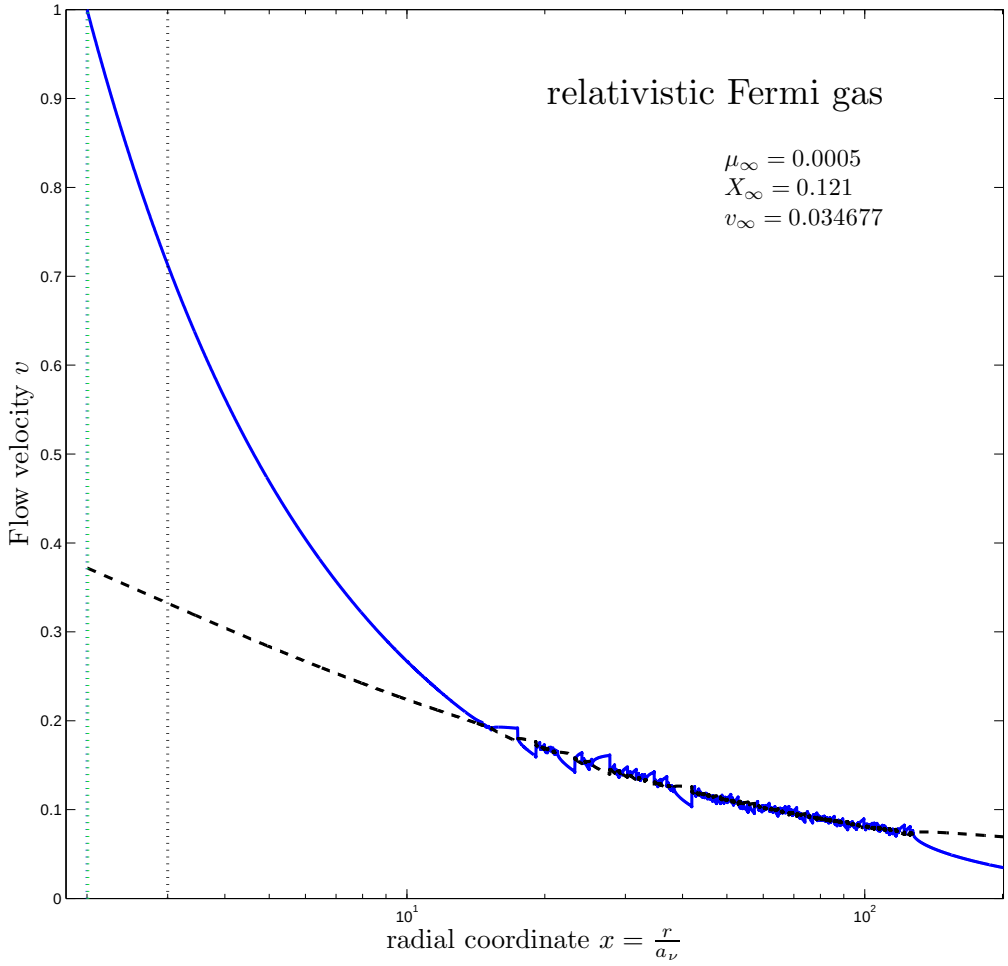

Figure 4.1: Flow velocity v (blue-solid) for a system of mass $M_\infty = 0.0005\ b_\nu \approx 9 \times 10^6 M_\odot$, with central mass fraction of $m_C = 0.9954$ alongside the speed of sound c_S (black-dashed).

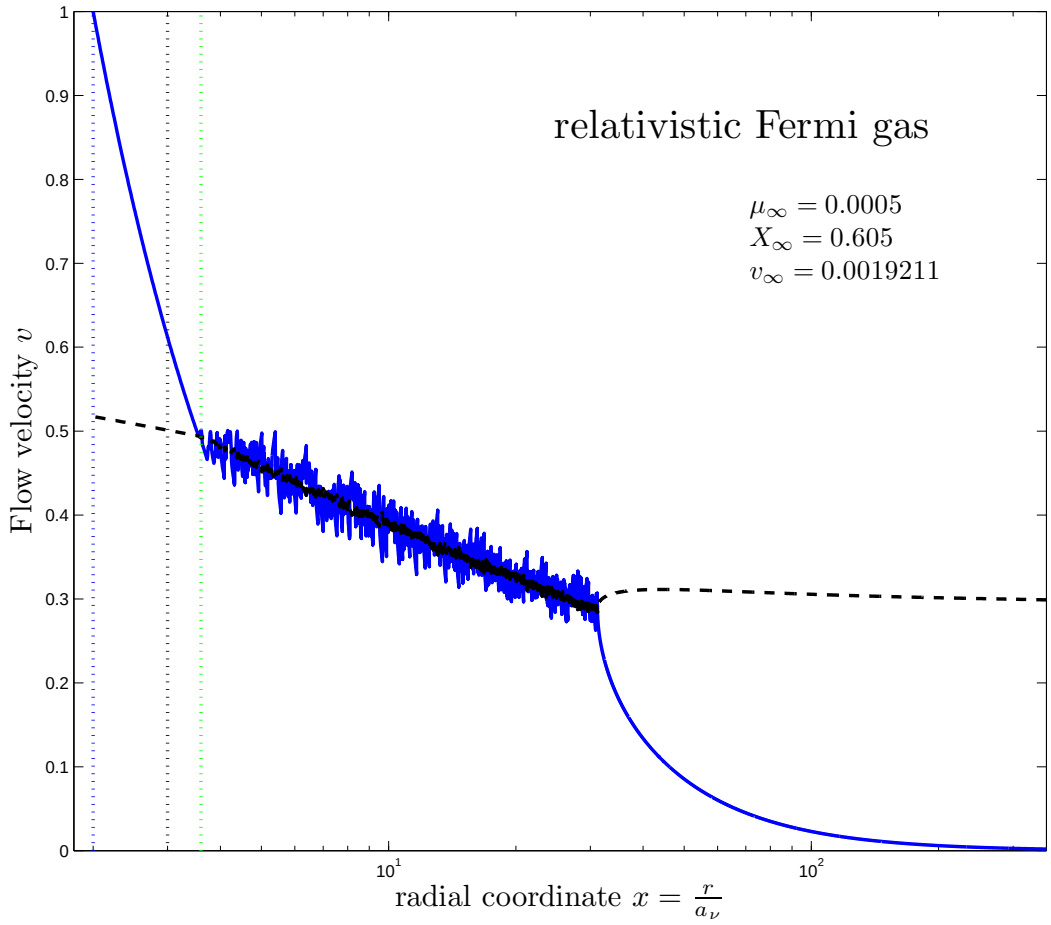

Figure 4.2: Flow velocity v (blue-solid) for a system of mass $M_\infty = 0.0005\ b_\nu \approx 9 \times 10^6 M_\odot$, with central mass fraction of $m_C = 0.5556$ alongside the speed of sound c_S (black-dashed).

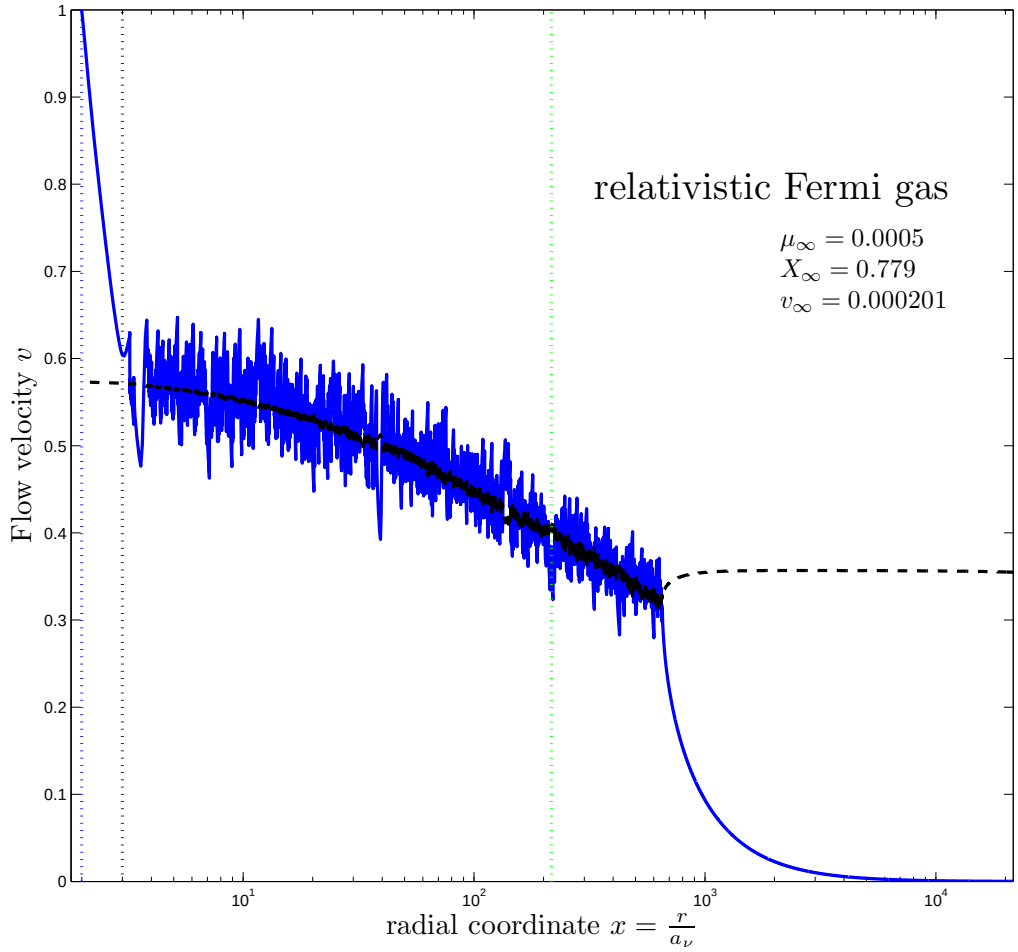

Figure 4.3: Flow velocity v (blue-solid) for a system of mass $M_\infty = 0.0005$ $b_\nu \approx 9 \times 10^6 M_\odot$, with central mass fraction of $m_C = 0.0092$ alongside the speed of sound c_S (black-dashed).

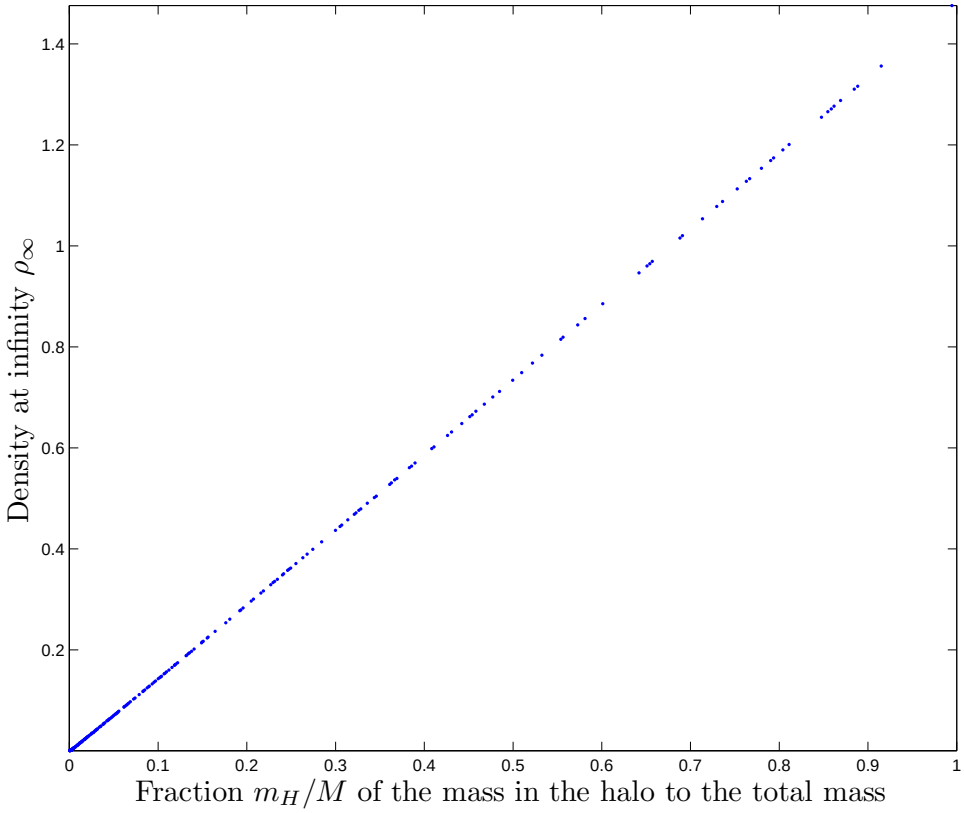

Figure 4.4: As with the previous model of polytropic accretion with $w = 1/3$, the relativistic accretion of a relativistic Fermi gas shows that the density at the observer, ρ_∞, is proportional to the mass of the halo surrounding the central body, m_H. The density axis is given in units of the constant k mentioned in the text.

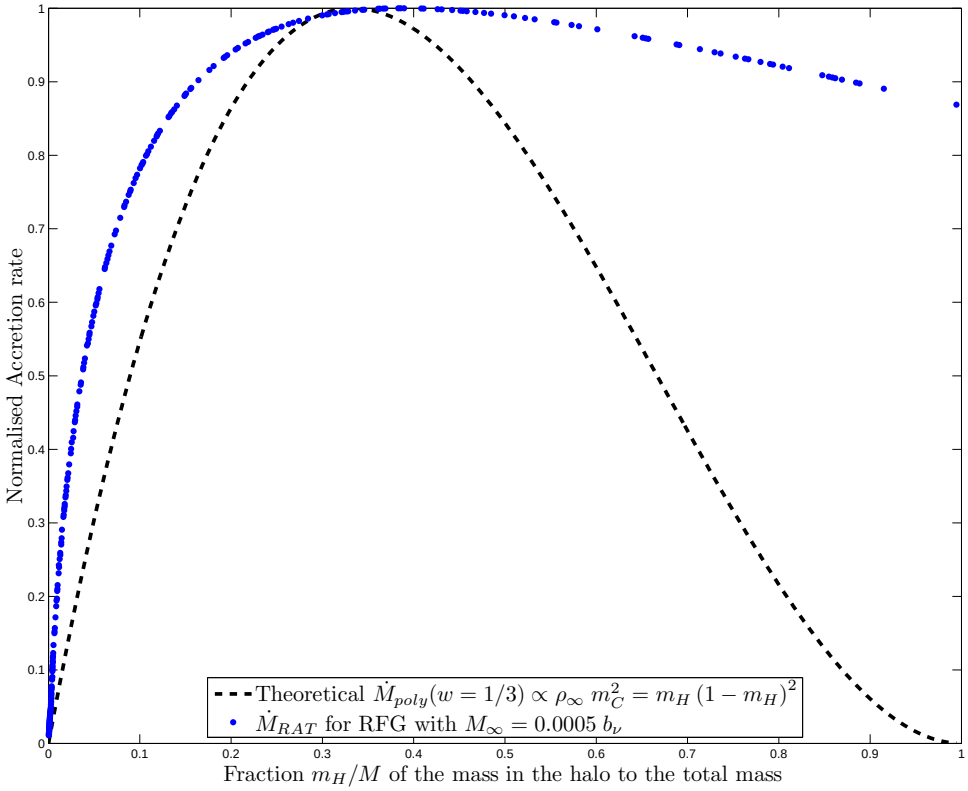

Figure 4.5: The relativistic Fermi gas accretion rate curve for a system of mass $\mu_\infty = 5 \times 10^{-4}$ or $M_\infty = 9.0843 \times 10^6 M_\odot$ (blue-dotted) behaves similarly to the rate from the accretion of the $w = 1/3$ polytropic fluid (black-dashed) in the test-fluid regime, but deviates from the latter's behaviour in the dominating halo regime. The curve peaks at $m_H = 0.4109$ with value of 0.1525 in units of γ_ν.

Chapter 5

Conclusion

A coherent, completely relativistic framework, that describes the spherical accretion of a self-gravitating fluid around a central accreting body, has been presented. The test cases of the polytropic fluids of ultra-relativistic stiff matter and radiation have yielded agreeable and feasible numerical results for the test-fluid scenarios [7], which serve as a link to the Bondi-type accretion neglecting the backreaction of the fluid on the surrounding spacetime. Furthermore, the radiation accretion rate compares well to that calculated by similar theories [9, 10] which include the all-important self-gravitation of the accreting fluid. Under these scrutinies, the proposed model behaves well and recreates familiar physics.

Furthermore, the model has been extended to work on a relativistic Fermi gas surrounding an accreting black hole, with promising results. The flow properties in this case compares relatively well with the test case for polytropic fluid accretion ($w = 1/3$). The preliminary calculations give an accretion timeframe of < 3 Myr for a solar mass seed black hole to grow to the scale of a $10^7 M_\odot$ SMBH, in accordance with the symbiotic scenario.

Further study is needed to explore the model's parameter space thoroughly, as systems with such non-linearity and many input parameters are difficult to explore and analyse.

Acknowledgements

I would like to thank my supervisor Prof. R.D. Viollier and co-supervisor Dr. G.B. Tupper as well as Prof. Andre Peshier for all their help and insight. I would also like to thank The National Research Foundation and the National Institute for Theoretical Physics for their financial support.

List of Figures

Bibliography

[1] F. Hoyle and R. A. Lyttleton, "On the Physical Aspects of Accretion by Stars," Proc. Cam. Phil. Soc. **36**, 424 (1940).

[2] R. A. Lyttleton and F. Hoyle, "The Evolution of the Stars," The Observatory **63**, 39 (1940).

[3] H. Bondi and F. Hoyle, "On the mechanism of accretion by stars," Mon. Not. Roy. Astron. Soc. **104**, 273 (1944).

[4] H. Bondi, "On spherical accretion," Mon. Not. Roy. Astron. Soc. **112**, 195 (1952).

[5] F. C. Michel, "Accretion of matter by condensed objects," Astrophys. Space Sci. **15**, 153 (1972).

[6] S. L. Shapiro and S. A. Teukolsky, *Black Holes, White Dwarfs and Neutron Stars* (Wiley-Interscience, New York, 1983).

[7] E. Babichev, V. Dokuchaev, and Y. Eroshenko, "Black Hole Mass Decreasing due to Phantom Energy Accretion," Phys. Rev. Lett. **93**, 021102 (2004).

[8] E. Babichev, V. Dokuchaev, and Y. Eroshenko, "The Accretion of Dark Energy onto a Black Hole," J.Exp.Theor.Phys. **100**, 528 (2005), astro-ph/0505618.

[9] B. Kinasiewicz, P. Mach, and E. Malec, "Selfgravitation in a general-relativistic accretion of steady fluids," Int. J. Geom. Meth. Mod. Phys **4**, 197 (2007), gr-qc/0606004.

[10] J. Karkowski, B. Kinasiewicz, P. Mach, E. Malec, and Z. Świerczyński, "Universality and backreaction in a general-relativistic accretion of steady fluids," Phys. Rev. **D73**, 021503(R) (2006).

[11] C. J. Willott, R. J. McLure, and M. J. Jarvis, "A 3 $\times 10^9$ solar mass black hole in the quasar SDSS J1148+5251 at $z = 6.41$," Astrophys. J. **587**, L15 (2003).

[12] M. C. Richter, G. B. Tupper, and R. D. Viollier, "A Symbiotic Scenario for the Rapid Formation of Supermassive Black Holes," JCAP **12**, 015 (2006), astro-ph/0611552.

[13] T. Asaka and M. Shaposhnikov, "The νMSM, dark matter and neutrino masses," Phys. Lett. **B631**, 151 (2005).

[14] T. Asaka and M. Shaposhnikov, "The νMSM, dark matter and baryon asymmetry of the universe," Phys. Lett. **B620**, 17 (2005).

[15] M. Shaposhnikov and I. Tkachev, "The νMSM, inflation and dark matter," Phys. Lett. **B639**, 414 (2006), hep-ph/0604236.

[16] P. B. Pal and L. Wolfenstein, "Radiative decays of massive neutrinos," Phys. Rev. **D25**, 766 (1982).

[17] G. Steigman, "Primordial nucleosynthesis: Success and challenges," Int. J. Mod. Phys. **E15**, 1 (2006).

[18] X. Shi and G. M. Fuller, "New dark matter candidate: Non-thermal sterile neutrinos," Phys. Rev. Lett. **82**, 2832 (1999).

[19] K. N. Abazajian, G. M. Fuller, and M. Patel, "Sterile neutrino hot, warm, and cold dark matter," Phys. Rev. **D64**, 023501 (2001).

[20] K. N. Abazajian and G. M. Fuller, "Bulk QCD thermodynamics and sterile neutrino dark matter," Phys. Rev. **D66**, 023526 (2002).

[21] K. N. Abazajian and S. M. Koushiappas, "Constraints on sterile neutrino dark matter," Phys. Rev. **D74**, 023527 (2006), astro-ph/0605271.

[22] S. Dodelson and L. M. Widrow, "Sterile neutrinos as dark matter," Phys. Rev. Lett. **72**, 17 (1994).

[23] R. Barbieri and A. D. Dolgov, "Bounds on sterile neutrinos from nucleosynthesis," Phys. Lett. **B237**, 440 (1990).

[24] K. Kainulainen, "Light singlet neutrinos and the primordial nucleosynthesis," Phys. Lett. **B244**, 191 (1990).

[25] M. Viel, J. Lesgourgues, M. G. Haehnelt, S. Matarrese, and A. Riotto, "Can sterile neutrinos be ruled out as warm dark matter candidates?," Phys. Rev. Lett. **97**, 1301 (2006), astro-ph/0605706.

[26] M. A. Markov, "On possible existence of neutrino superstars," Phys. Lett. **10**, 122 (1964).

[27] R. Ruffini, "On a system of self-gravitating Fermi-degenerate neutrinos," Lett. Nuovo Cim. **29**, 161 (1980).

[28] R. D. Viollier, D. Trautmann, and G. B. Tupper, "Supermassive neutrino stars and galactic nuclei," Phys. Lett. **B306**, 79 (1993).

[29] F. Munyaneza, D. Tsiklauri, and R. D. Viollier, "Sgr A*: A supermassive black hole or a spatially extended object?," Astrophys. J. **509**, L105 (1998).

[30] F. Munyaneza, D. Tsiklauri, and R. D. Viollier, "Dynamics of the star S0-1 and the nature of the compact dark object at the galactic center," Astrophys. J. **526**, 744 (1999).

[31] J. R. Oppenheimer and G. M. Volkoff, "On massive neutron cores," Phys. Rev. **55**, 374 (1939).

[32] N. Bilić, F. Munyaneza, and R. D. Viollier, "Stars and halos of degenerate relativistic heavy-neutrino and neutralino matter," Phys. Rev. **D59**, 024003 (1999).

[33] L. Landau and E. Lifshitz, *The Classical Theory of Fields* (Addison-Wesley Publishing Company, 1951).

[34] R. C. Tolman, *Relativity, Thermodynamics and Cosmology* (Clarendon Press, Oxford, 1934).